

Thermoelectric property studies on thallium-doped lead telluride prepared by ball milling and hot pressing

Bo Yu,¹ Qinyong Zhang,¹ Hui Wang,¹ Xiaowei Wang,¹ Hengzhi Wang,¹ Dezhi Wang,¹ Heng Wang,² G. Jeffrey Snyder,² Gang Chen,^{3,a)} and Z. F. Ren^{1,a)}

¹Department of Physics, Boston College, Chestnut Hill, Massachusetts 02467, USA

²Department of Materials Science, California Institute of Technology, Pasadena California 91125, USA

³Department of Mechanical Engineering, Massachusetts Institute of Technology, Cambridge, Massachusetts 02139, USA

(Received 12 March 2010; accepted 15 May 2010; published online 12 July 2010)

Thallium doping into lead telluride has been demonstrated to increase the dimensionless thermoelectric figure-of-merit (ZT) by enhancing Seebeck coefficient due to the creation of resonant states close to Fermi level without affecting the thermal conductivity. However, the process is tedious, energy consuming, and small in quantities since it involves melting, slow cooling for crystal growth, long time annealing, post-crushing and hot pressing. Here we show that a similar ZT value about 1.3 at 400 °C is achieved on bulk samples with grain sizes of 3–7 μm by ball milling a mixture of elemental thallium, lead, and tellurium and then hot pressing the ball milled nanopowders. © 2010 American Institute of Physics. [doi:10.1063/1.3452323]

Thermoelectrics (TEs), as one of the most promising approaches for solid-state energy conversion between heat and electricity, is becoming increasingly important within the last decade as the availability and negative environmental impact of fossil fuels draw increasing attention. Various TE materials with a wide working temperature range (from 25 to 1000 °C) for different applications in cooling and power generation have been extensively studied. The efficiency of TE devices is determined by a dimensionless figure-of-merit $ZT=(S^2\sigma/\kappa)T$, where S is the Seebeck coefficient, σ the electrical conductivity, κ the thermal conductivity (sum of the electronic part κ_e and the lattice part κ_L), and T the absolute temperature of the material.¹

Lead telluride (PbTe) is one of the most studied and used intermediate temperature TE materials with a ZT of about 1 at 380 °C,² which is suitable for power generation applications such as waste heat recovery³ and potentially in solar energy conversion.⁴ However, the toxicity of Pb is a big concern, which slowed down the applications of such materials. Nevertheless, the interest in PbTe has significantly increased due to the demonstration of a ZT higher than 1.5 by creating nanosized inclusions in bulk crystalline materials (lead antimony silver telluride) using the traditional crystal growth technique, in which the improvement comes from thermal conductivity reduction due to the increased phonon scattering by the nanosized inclusions in the materials.⁵ The formation of such inclusions is believed to be caused by substituting some Pb with Ag and Sb.

Recently, a ZT of about 1.5 at around 500 °C was also reported through improving the Seebeck coefficient⁶ via creating resonant states close to Fermi level by using a 2 at. % thallium (Tl) to replace Pb (Tl_{0.02}Pb_{0.98}Te). However, the process is very tedious since it involves melting, slow cooling for crystal growth, long time annealing, post-crushing, and hot pressing for compacting the powders into dense bulk samples. Such a slow process is not practical to large scale

production of multiple tons per year required by industrial applications.

In the last few years, we have successfully demonstrated that large quantities of bulk nanostructured TE materials can be easily produced by ball milling and hot pressing either ingots⁷ or elements,^{8–12} in a short time without involving the tedious melting and slow cooling for crystal growth. It would be very beneficial if such a simple process can be applied to the Tl_{0.02}Pb_{0.98}Te system to create nanosized grains and nanostructures so that thermal conductivity can be significantly reduced, leading to further ZT enhancement. In this paper, we report our study on using ball milling and hot pressing technique to make dense bulk Tl_{0.02}Pb_{0.98}Te samples and their TE properties.

Tl_{0.02}Pb_{0.98}Te nanopowders were prepared by ball milling Pb (99.999%, Alfa Aesar), Te (99.99%, EZMetals Corp., Canada), and Tl (99.999%, Alfa Aesar) in a ball mill jar with balls made of stainless steel. After about 10–20 h ball milling, Tl_{0.02}Pb_{0.98}Te alloy powders were formed. These alloyed powders were then loaded into a graphite die and compacted into dense bulk disks of either 12.7 or 25.4 mm in diameter through direct current induced hot press (dc hot press). The materials were handled in a glove box filled with argon gas to minimize contaminations. After press, a sample density of about 8.1–8.2 g/cm³ was obtained which is almost the same as that of the bulk PbTe (8.16 g/cm³). The hot-pressed bulk samples were then measured by multiprobe transport system (ULVAC-RIKO ZEM-3) for electrical conductivity and Seebeck coefficient and laser flash (Netzsch LFA457) for thermal conductivity. Various samples were also measured using the systems described in Ref. 6 yielding consistent results. The microstructure of the as-prepared nanopowders and bulk samples were characterized by x-ray diffraction (XRD, Bruker-AXS, G8 GAADS) using Cu target ($K\alpha$, $\lambda = 0.154$ nm), scanning electron microscope (SEM, JEOL-6340F), and transmission electron microscope (TEM, JEOL-2010F).

^{a)}Electronic mail: renzh@bc.edu, gchen2@mit.edu.

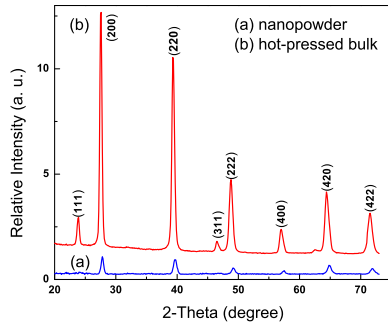


FIG. 1. (Color online) XRD spectra for the ball milled nanopowders $\text{Tl}_{0.02}\text{Pb}_{0.98}\text{Te}$ (a) and the hot-pressed dense bulk samples $\text{Tl}_{0.02}\text{Pb}_{0.98}\text{Te}$ (b).

Figure 1 shows the XRD spectra of the ball milled $\text{Tl}_{0.02}\text{Pb}_{0.98}\text{Te}$ nanopowders [Fig. 1(a)] and the hot-pressed dense bulk samples [Fig. 1(b)]. It confirmed that all the three elements Tl, Pb, and Te were fully alloyed after ball milling of about 10 to 20 h since all the peaks were indexed according to those of the PbTe phase and no peaks belong to Tl or Pb or Te. It is clear that all the peaks of the ball milled powders were weak [Fig. 1(a)] but very sharp and intense [Fig. 1(b)] for the hot-pressed dense bulk samples because of the larger grain size. Also, another noticeable feature we can see from the pattern comparison is the small peak shift in the nanopowder to a higher angle, meaning a smaller lattice parameter. We attribute this to the stress built-up in the nanopowder during ball milling.

The as-prepared nanopowders were dispersed with ultrasonics in methanol and then dried and fixed to carbon film on copper grid. As shown in Figs. 2(a) and 2(b) [enlargement of the square box in Fig. 2(a)], bright field TEM micrographs of the powders showed that the particles are around 20–50 nm in size, although most of the powders aggregated or overlapped in the images. The selected area electron diffraction (SAED) pattern [Fig. 2(c)] showed that most of the particles

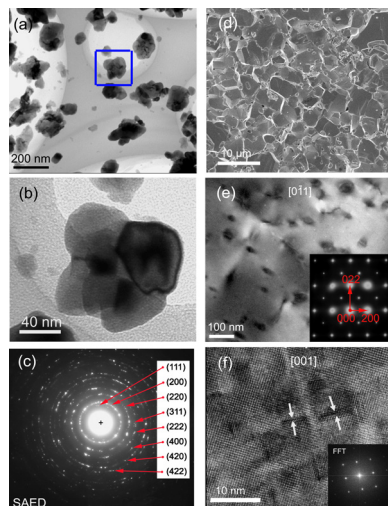


FIG. 2. (Color online) Low (a) and high (b) magnification TEM images, and SAED patterns (c) of the ball milled nanopowders $\text{Tl}_{0.02}\text{Pb}_{0.98}\text{Te}$; SEM image (d), TEM image taken with the incident electron beam along $[0\bar{1}1]$ (e) (indexed SAED pattern shown as the inset) and $[001]$ direction (f) of the hot-pressed dense bulk samples $\text{Tl}_{0.02}\text{Pb}_{0.98}\text{Te}$, the arrows point out the positions of the disks. (FFT pattern in the inset shows the $[001]$ zone axis.)

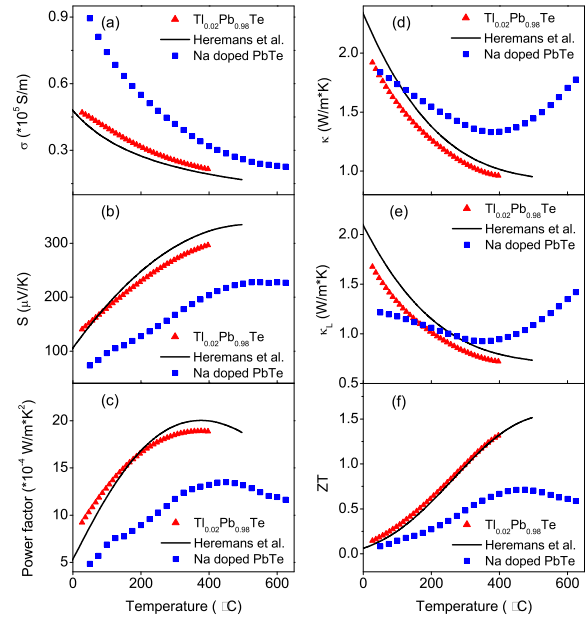


FIG. 3. (Color online) (a) Electrical conductivity σ , (b) Seebeck coefficient S , (c) power factor, (d) thermal conductivity κ , (e) lattice thermal conductivity κ_L , and (f) dimensionless figure-of-merit ZT dependence of temperature of the hot-pressed dense bulk samples $\text{Tl}_{0.02}\text{Pb}_{0.98}\text{Te}$ (Ref. 19) and a reference sample (Ref. 20) of Na doped p-type PbTe in comparison with the reference data (Ref. 6).

were well crystallized/alloyed during ball milling, consistent with the XRD spectra shown in Fig. 1(a).

Figure 2(d) shows an SEM image of the freshly broken surface of the hot-pressed sample, which clearly demonstrates that most of the grain size is in the range of 3–7 μm , much larger than the original particle size of less than 50 nm right after ball milling [Fig. 2(b)], which indicates that the crystal growth or coalescence of the nanoscaled PbTe grains is fairly significant during hot pressing. The large grain size is not what we intended to achieve. It is still a challenge to prevent the grain growth in this material, which is being studied in our group.

There have been extensive reports on microstructures on PbTe systems^{5,13–17} by TEM. It was generally suggested that there are lots of nanoscaled endotaxial precipitates or nano-inclusions embedded in the matrix, which was believed to be one of the reasons for the lower thermal conductivity and enhanced ZT values. As shown in Fig. 2(e), when the specimen was projected along $[0\bar{1}1]$ direction (the indexed SAED pattern was shown as the inset), the dark disks look like nano-inclusions as reported. However, our recent TEM observations showed that they are not precipitates or nano-inclusions but lattice-strain fields, originated from nanoscaled Pb-depleted disks lying on $\{001\}$ planes. High-resolution TEM microphotograph in Fig. 2(f) clearly showed the vacancy disks, around 2–5 nm in diameter, indicated by the white arrows, and the related strain fields on both sides of the disks, when the specimen was oriented along the $[001]$ zone axis [see the fast Fourier transform (FFT) pattern as the inset in Fig. 2(f)]. The detailed analysis of these defect disks and their strain fields will be reported in a separate paper.¹⁸

Figure 3 shows the TE properties¹⁹ in comparison with results from the original report on $\text{Tl}_{0.02}\text{Pb}_{0.98}\text{Te}$ (Ref. 6) and

a reference PbTe sample²⁰ doped with Na. Our samples have a slightly higher electrical conductivity [Fig. 3(a)] and a slightly lower Seebeck coefficient [Fig. 3(b)] probably due to a little bit higher carrier concentration caused by higher defect density resulting from the ball milling process. The Seebeck coefficients of about 150 $\mu\text{V}/\text{K}$ at 25 °C and 300 $\mu\text{V}/\text{K}$ at 400 °C are much higher than those of the Na doped PbTe sample, which confirms the benefit of adding Tl to partially replace Pb in the PbTe system. As a result of the enhanced Seebeck coefficient, we achieved a similar power factor as reported in Ref. 6 [Fig. 3(c)] but higher than that of Ref. 17 despite of the lower electrical conductivity. Interestingly, our samples also showed a little bit lower thermal conductivity [Fig. 3(d)] even though the grain size is large (3–7 μm), which leads to a similar ZT dependence of temperature up to 400 °C with the reported values [Fig. 3(f)]. It is worth pointing out that we did not measure beyond 400 °C due to the sample softening problem we encountered. Such similar ZT results clearly demonstrate that ball milling and hot pressing process is applicable to the Tl-doped PbTe system. The highest ZT value of 1.3 was achieved at about 400 °C.

The Lorenz number L was calculated²¹ from the original formula based on the Boltzmann transport equation for electrons

$$L = \left(\frac{k_B}{e} \right)^2 \left\{ \frac{(s+7/2)F_{s+5/2}(\xi)}{(s+3/2)F_{s+1/2}(\xi)} - \left[\frac{(s+5/2)F_{s+3/2}(\xi)}{(s+3/2)F_{s+1/2}(\xi)} \right]^2 \right\}, \quad (1)$$

where $F_n(\xi) = \int_0^\infty [\chi^n / (1 + e^{\chi - \xi})] d\chi$ is the Fermi integral and ξ is the reduced Fermi energy. Since carrier concentrations are unavailable, we, therefore, derived the reduced Fermi energy from Seebeck coefficient at room temperature while the values at other temperatures could be calculated from the defined formula $\xi = E_F / k_B T$. Then by using Wiedemann–Franz law ($\kappa_e = L\sigma T$), we estimated the lattice thermal conductivity κ_L by subtracting the electronic part κ_e and found that our samples have a little bit lower lattice thermal conductivity in comparison with the report.⁶ We believe that the higher defect disks (coherent interfaces) and the lattice-strain fields¹⁸ may have played an important role on the stronger phonon scattering, leading to the reduction in lattice thermal conductivity [Fig. 3(e)].^{5,22,23}

Clearly the grain size in our dense bulk samples is not less than 100 nm due to the significant grain growth during hot pressing even though we planned to have the grains smaller than 100 nm. Therefore, it is reasonable to expect that a much lower thermal conductivity would be achieved if the grain size could be made less than 100 nm. How to prevent the grain growth in PbTe system is apparently very challenging. When an appropriate approach is found to achieve grain size less than 100 nm in the future, we expect to have thermal conductivity much lower than the current values. So it is hopeful that a peak ZT value of above 2 at about 400 °C is possible in Tl-doped PbTe system. However, a bigger challenge is to make the materials mechanically strong above 400 °C so that any potential applications can be explored.

In summary, we have successfully demonstrated that the simple ball milling and hot pressing technique is applicable to the $\text{Tl}_{0.02}\text{Pb}_{0.98}\text{Te}$ system to achieve ZT values about 1.3 at 400 °C even though the samples soften at above 400 °C. Further improvement on ZT may be possible if the grain size could be less than 100 nm and more work needs to be done on enhancing the mechanical strength at above 400 °C.

The work on sample preparation and characterizations is funded by the U.S. Department of Energy, Office of Science, and Office of Basic Energy Sciences under Award No. DE-FG02-08ER46516 (M.S.D., G.C., and Z.F.R.), and some of the transport measurements were performed at Caltech funded by BSST, California (G.J.S.).

- ¹D. M. Rowe, in *CRC Handbook of Thermoelectrics*, edited by D. M. Rowe (CRC, Boca Raton, Florida, 2006), pp. 1–10.
- ²Y. I. Ravich, B. A. Efimova, and I. A. Smirnov, *Semiconducting Lead Chalcogenides*, Monographs in Semiconductor Physics Vol. 5 (Plenum, New York, 1970).
- ³T. Caillat, J. Fleurial, and A. Borshchevsky, *AIP Conf. Proc.* **420**, 1647 (1998).
- ⁴R. J. Campana, *Adv. Ener. Conv.* **2**, 303 (1962).
- ⁵K. F. Hsu, S. Loo, F. Guo, W. Chen, J. S. Dyck, C. Uher, T. Hogan, E. K. Polychroniadis, and M. G. Kanatzidis, *Science* **303**, 818 (2004).
- ⁶J. P. Heremans, V. Jovovic, E. S. Toberer, A. Saramat, K. Kurosaki, A. Charoenphakdee, S. Yamanaka, and G. J. Snyder, *Science* **321**, 554 (2008).
- ⁷B. Poudel, Q. Hao, Y. Ma, Y. C. Lan, A. Minnich, B. Yu, X. Yan, D. Z. Wang, A. J. Muto, D. Vashaee, X. Y. Chen, J. M. Liu, M. S. Dresselhaus, G. Chen, and Z. F. Ren, *Science* **320**, 634 (2008).
- ⁸Y. Ma, Q. Hao, B. Poudel, Y. C. Lan, B. Yu, D. Z. Wang, G. Chen, and Z. F. Ren, *Nano Lett.* **8**, 2580 (2008).
- ⁹X. W. Wang, H. Lee, Y. C. Lan, G. H. Zhu, G. Joshi, D. Z. Wang, J. Yang, A. J. Muto, M. Y. Tang, J. Klatsky, S. Song, M. S. Dresselhaus, G. Chen, and Z. F. Ren, *Appl. Phys. Lett.* **93**, 193121 (2008).
- ¹⁰G. Joshi, H. Lee, Y. C. Lan, X. W. Wang, G. H. Zhu, D. Z. Wang, R. W. Gould, D. C. Cuff, M. Y. Tang, M. S. Dresselhaus, G. Chen, and Z. F. Ren, *Nano Lett.* **8**, 4670 (2008).
- ¹¹G. H. Zhu, H. Lee, Y. C. Lan, X. W. Wang, G. Joshi, D. Z. Wang, J. Yang, D. Vashaee, H. Guilbert, A. Pillitteri, M. S. Dresselhaus, G. Chen, and Z. F. Ren, *Phys. Rev. Lett.* **102**, 196803 (2009).
- ¹²J. Yang, Q. Hao, H. Wang, Y. C. Lan, Q. Y. He, A. J. Minnich, D. Z. Wang, J. A. Harriman, V. M. Varki, M. S. Dresselhaus, G. Chen, and Z. F. Ren, *Phys. Rev. B* **80**, 115329 (2009).
- ¹³P. F. P. Poudeu, J. J. D'Angelo, A. D. Downey, J. L. Short, T. P. Hogan, and M. G. Kanatzidis, *Angew. Chem., Int. Ed.* **45**, 3835 (2006).
- ¹⁴J. Androulakis, K. F. Hsu, R. Pcionek, H. Kong, C. Uher, J. J. D'Angelo, A. Downey, T. Hogan, and M. G. Kanatzidis, *Adv. Mater.* **18**, 1170 (2006).
- ¹⁵J. Androulakis, C. Lin, H. Kong, C. Uher, C. Wu, T. Hogan, B. A. Cook, T. Caillat, K. M. Paraskevopoulos, and M. G. Kanatzidis, *J. Am. Chem. Soc.* **129**, 9780 (2007).
- ¹⁶M. Zhou, J.-F. Li, and T. Kita, *J. Am. Chem. Soc.* **130**, 4527 (2008).
- ¹⁷P. F. P. Poudeu, A. Gu'eguen, C.-I. Wu, T. Hogan, and M. G. Kanatzidis, *Chem. Mater.* **22**, 1046 (2010).
- ¹⁸H. Z. Wang, Q. Y. Zhang, B. Yu, H. Wang, W. S. Liu, D. Z. Wang, G. Chen, and Z. F. Ren, "TEM study of Pb-depleted discs in PbTe-based alloys," *Philos. Mag. Lett.* (submitted).
- ¹⁹Y. C. Lan, A. Minnich, G. Chen, and Z. F. Ren, *Adv. Funct. Mater.* **20**, 357 (2010).
- ²⁰R. W. Fritts, in *Thermoelectric Materials and Devices*, edited by I. B. Cadoff and E. Miller (Reinhold, New York, 1960), pp. 143–162.
- ²¹W. S. Liu, B. P. Zhang, J. F. Li, H. L. Zhang, and L. D. Zhao, *J. Appl. Phys.* **102**, 103717 (2007).
- ²²E. Quarez, K.-F. Hsu, R. Pcionek, N. Frangis, E. K. Polychroniadis, and M. G. Kanatzidis, *J. Am. Chem. Soc.* **127**, 9177 (2005).
- ²³B. A. Cook, M. J. Cramer, J. L. Harringa, M. K. Han, D. Y. Chung, and M. G. Kanatzidis, *Adv. Funct. Mater.* **19**, 1254 (2009).